Journal of Catalysis 279 (2011) 233–240

Contents lists available at ScienceDirect

Journal of Catalysis

journal homepage: www.elsevier.com/locate/jcat

Efficient and selective formation of methanol from methane in a fuel cell-type reactor

Byungik Lee, Takashi Hibino *

Graduate School of Environmental Studies, Nagoya University, Guro-cho, Chikusa-ku, Nagoya 464-8601, Japan

ARTICLE INFO

Article history:
Received 22 October 2010
Revised 10 December 2010
Accepted 27 December 2010

Keywords:
Methane oxidation
Methanol synthesis
Active oxygen species
Fuel cell-type reactor

ABSTRACT

Direct oxidation of methane to methanol at low temperatures was investigated using a fuel cell-type reactor, where a mixture of methane and H_2O vapor was supplied to the anode and air to the cathode. Methanol was scarcely produced over a Pt/C anode from 50 to 250 °C. However, through trial and error, the production of methanol over a V_2O_5/SnO_2 anode was significant at 100 °C; the current efficiency for methanol production and the selectivity toward methanol were as high as 61.4% and 88.4%, respectively. Methanol was produced by the reaction of methane with an active oxygen species over the V_2O_5 catalyst. Cyclic voltammetry of the anode indicated that the generation of such active oxygen species was strongly dependent on the anode potential. Moreover, X-ray diffraction, transmission electron microscopy, and X-ray photoelectron spectroscopy measurements confirmed that highly dispersed and partially reduced vanadium species were present on the SnO_2 surface. These vanadium species are considered to be active sites for the formation of the active oxygen species, probably anion radicals (O_2^- and $O^{\cdot -}$).

1. Introduction

While there have been considerable efforts in oxidizing methane to methanol in a one-pass process over solid catalysts [1–5], this process has not yet been realized in practical applications, because (a) methane is a very inert reactant, requiring high reaction temperatures (in many cases, $T > 400$ °C), and (b) methanol is an intermediate product, making it difficult to achieve high selectivity at high methane conversion. As part of the search for an alternative approach to the direct oxidation of methane to methanol, we have applied an electrochemical cell to the reaction system. In our previous studies, methane could be converted into methanol using a proton-conducting fuel cell capable of operation at 100 °C or higher [6,7]. Methane oxidation was performed by the active oxygen species generated at the cathode:

$$\text{Anode}: \quad H_2 \rightarrow 2H^+ + 2e^- \tag{1}$$

$$\text{Cathode}: \quad O_2 + 2H^+ + 2e^- \rightarrow (H_2O_2) \rightarrow O^* + H_2O \tag{2}$$

$$CH_4 + O^* \rightarrow CH_3OH \tag{3}$$

Significant production of methanol and CO_2 over a PdAu/C cathode was achieved. Furthermore, the addition of CuO to PdAu increased the formation rate of methanol and decreased the formation rate of CO_2. However, this approach has a serious challenge in that the current efficiency for methanol production is only 0.013%, because the predominant cathode reaction is not Reaction (2), but Reaction (4):

$$\text{Cathode}: \quad O_2 + 4H^+ + 4e^- \rightarrow 2H_2O \tag{4}$$

One approach to overcome this challenge is to supply a mixture of methane and H_2O vapor to the anode and air to cathode, which can be regarded as a direct methane fuel cell. We previously reported the direct oxidation of methane over a Pt/C anode in the temperature range of 100–300 °C, where methane reacts with an active oxygen species, HO, to form CO_2 during the cell discharge [8]. It is also worth noting that as the temperature increased, the concentration of CO_2 produced became closer to the theoretical value calculated from Faraday's law, according to the following reaction:

$$\text{Anode}: \quad CH_4 + 2H_2O \rightarrow CO_2 + 8H^+ + 8e^- \tag{5}$$

Therefore, if the oxidation ability of the active oxygen species for methane is reduced, then selective oxidation of methane to methanol could be achieved while maintaining high current efficiency:

$$\text{Anode}: \quad CH_4 + H_2O \rightarrow CH_3OH + 2H^+ + 2e^- \tag{6}$$

This may be accomplished by using a metal or metal oxide catalyst that is more inert than Pt. In addition, it may be important to replace carbon with a semiconducting metal oxide, since the active oxygen species is stabilized not only on the Pt surface, but also on the carbon surface [9].

* Corresponding author. Fax: +81 52 789 4894.
E-mail address: hibino@urban.env.nagoya-u.ac.jp (T. Hibino).

0021-9517/$ - see front matter © 2010 Elsevier Inc. All rights reserved.
doi:10.1016/j.jcat.2010.12.020

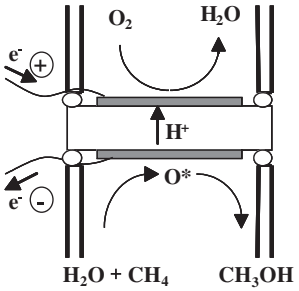

Scheme 1. Schematic illustration of the fuel cell-type reactor.

Based on these observations and assumptions, it is expected that an electrochemical reactor for methanol synthesis can be developed through Reactions (6) and (4), as illustrated in Scheme 1. (Although a similar concept was proposed in US Patent No. 5051,156 [10], the current efficiency reported was as low as 6.1%, which is still insufficient for practical applications.) The goals of the present work are to (1) enhance the current efficiency for methanol production by employing a more promising catalyst and support and (2) clarify the reaction mechanism by various means, including electrochemical, kinetic, and spectroscopic techniques.

2. Experimental

2.1. Materials

Proton conductors are important for the study described here. The proton conductor used was $Sn_{0.9}In_{0.1}P_2O_7$ because this material possesses proton conductivity above 0.1 S cm^{-1} in the temperature range of 100–300 °C [11]. SnO_2 and In_2O_3 were mixed with 85% H_3PO_4 and de-ionized water. The mixture was stirred at 300 °C until the mixture formed a high viscosity paste. The paste was calcined in a covered alumina crucible at 650 °C for 2.5 h and then ground with a mortar and pestle. The characteristics of $Sn_{0.9}In_{0.1}P_2O_7$, including the electrochemical properties, crystalline structure, and composition, have been presented elsewhere [12].

For the preparation of the electrodes, three procedures were performed in the following order. First, various metal oxide supports (SnO_2, TiO_2, ZrO_2, CeO_2, WO_3, Fe_2O_3, and MoO_3) were impregnated with a 1 wt.% Mn_2O_3 catalyst. An appropriate quantity of $Mn(NO_3)_2{\cdot}6H_2O$ was stirred with each one of the supports in deionized water at 130 °C. After complete evaporation of water, the residue was recovered and then heated in Ar at 450 °C for 2 h. Next, 1 wt.% of various metals (Pd, Ru, Au, and Ag) or metal oxides (V_2O_5, Fe_2O_3, CoO, Mn_2O_3, MoO_3, and CrO) were impregnated on the surface of the optimized support. Impregnation of the catalysts was conducted using the corresponding metal salts (nitrates or chlorides) in the same manner as that for the Mn_2O_3 catalyst, although the metal catalysts were finally heated in 10 vol.% H_2 diluted with Ar at 450 °C for 2 h. Finally, the content of the optimized catalyst was changed from 0.5 to 1.5 wt.%. In all experiments, the catalyst/support powder was mixed with a polytetrafluoroethylene (PTFE) binder in a glycerin solvent using a mortar and pestle. The mixture was coated on the surface of a gas diffusion layer (Toray, TGPH-090), followed by heating in an Ar flow at 350 °C for 1 h.

2.2. Characterization

The BET surface areas of the metal oxide supports were measured using a Micromeritics automated system. All samples were degassed under vacuum at 100 °C for 1 h and then 250 °C for 3 h prior to BET surface area measurements. The catalyst/support powders were further characterized using X-ray diffraction (XRD), transmission electron microscopy (TEM), and X-ray photoelectron spectroscopy (XPS). The XRD patterns were recorded using a Rigaku Miniflex II diffractometer with Cu Kα radiation (λ = 1.5432 Å) operated at 45 kV and 20 mA. Powder diffraction patterns were recorded in the 2θ range from 10° to 90°. Specimens for TEM measurements were prepared by ultrasonic dispersion in *n*-butanol, and a drop of the suspension was evaporated on a Cu grid. Bright-field transmission images were obtained using a JEOL JEM2100F, which was equipped with a JEOL JED-2300T energy-dispersive X-ray (EDX) detector. XPS analysis was conducted using a VG Escallab220i-XL with an Al Kα (1486.6 eV) X-ray source. The photoemission angle was set at 45° to the sample surface, allowing for a reduction in the escape depth to several nanometers.

2.3. Electrochemical studies

The $Sn_{0.9}In_{0.1}P_2O_7$ powder was pressed into pellets (Ø12 × 1 mm) under a pressure of 200 MPa. A commercially available Pt/C cathode (1 mg Pt cm^{-2}) was obtained from BASF. The anode and cathode (area: 0.5 cm^2) were arranged on opposite faces of the electrolyte pellet. Two gas chambers were prepared by placing the cell assembly between two alumina tubes. Unless otherwise stated, the anode and cathode chambers were supplied with a mixture of 10% methane and 1% H_2O (Ar balance) and air, respectively, at a flow rate of 30 mL min^{-1}. Constant current was applied to the cell using a Hokuto Denko HA-501 galvanostat. The potential of the anode versus cathode was recorded with a Hokuto Denko HE-101 electrometer. The outlet gas from the anode chamber was analyzed using two online gas chromatographs with Shimadzu GC-2014 flame ionization and Varian CP-4900 thermal conductivity detectors. The entire gas line was heated at approximately 80 °C, and the gas concentrations were obtained after steady state was attained. The theoretical concentrations of methanol, CO_2, O_2, and CO products in the outlet gas from the anode chamber were calculated from Faraday's law based on two-, eight-, four-, and six-electron reactions, respectively. For example, the theoretical methanol concentration was calculated as follows:

$$V_{CH_3OH} = \frac{I \times 60}{2 \times F} \times 22,400 \times \frac{293}{273} \quad (7)$$

$$C_{CH_3OH} = \frac{V_{CH_3OH}}{V_{\text{outlet gas}}} \times 100 \quad (8)$$

where V_{CH_3OH}, I, F, C_{CH_3OH}, and $V_{\text{outlet gas}}$ denoted the flow rate of methanol produced (mL min^{-1}), current, (A), Faraday's constant, theoretical methanol concentration (%), and total flow rate of the outlet gas (mL min^{-1}), respectively. (We assumed that the flow rate of the outlet gas remained unchanged after methane oxidation.) Furthermore, the selectivity toward methanol, S_{CH_3OH}, and the current efficiency for methanol production, E_{CH_3OH}, were determined by using the following equations:

$$S_{CH_3} = \frac{\text{Observed } CH_3OH \text{ concentration}}{\text{Total product concentration}} \times 100 \quad (9)$$

$$E_{CH_3OH} = \frac{\text{Observed } CH_3OH \text{ concentration}}{\text{Theoretical } CH_3OH \text{ concentration}} \quad (10)$$

Further detailed characteristics of the anode were obtained using cyclic voltammetry (CV) with 10% methane and 1% H_2O (Ar balance) supplied to the anode at a flow rate of 30 mL min^{-1}. CV profiles were collected between −0.8 and +1.5 V at a scan rate of 3 mV s^{-1} (Hokuto Denko, HZ-5000).

3. Results and discussion

3.1. Methane oxidation over Pt/C

Electrochemical methane oxidation was first inspected over a Pt/C anode (4 mg Pt cm^{-2}) in a feed mixture of methane and H_2O vapor (Ar balance) at various temperatures. Different oxidation currents were applied to the anode at temperatures from 50 to 250 °C. Fig. 1a and b shows the potential of the anode versus cathode and the decrement in methane concentration, respectively, as a function of current. The anode potential at 0 mA became more negative as the temperature increased (Fig. 1a), which is interpreted as indicative that this electrochemical cell functions as a direct methane fuel cell. However, the anode potential was significantly shifted to the positive side by an increase in the current, due to the large internal electrical resistance of the cell. This means the transference from the fuel cell mode to the electrolysis mode. On the other hand, the methane concentration decreased with increasing current, and this effect became larger as the temperature increased (Fig. 1b). Considering that methane remained unreacted under open-circuit conditions, even at 250 °C, it is evident that the oxygen species generated electrochemically at the Pt/C anode has a very high activity for methane oxidation.

To better understand the observed electrochemical methane oxidation, the products in the outlet gas from the anode chamber at each temperature were analyzed. Table 1 shows that CO_2 and O_2 were the major products; the CO_2 concentration increased while the O_2 concentration decreased with increasing temperature, which indicates that Reaction (5) competes with Reaction (11), and this is dependent on the temperature.

$$\text{Anode}: \quad 2H_2O \rightarrow O_2 + 4H^+ + 4e^- \tag{11}$$

It should be kept in mind that the total CO_2 and O_2 concentrations at each current were less than the theoretical CO_2 and O_2 concentrations for 100% faradic efficiency. This discrepancy can be explained by the p-type semiconduction in the $Sn_{0.9}In_{0.1}P_2O_7$ electrolyte, because this material is not a pure proton conductor under fuel cell conditions [12]. Importantly, Table 1 also revealed that methanol was produced at 100 °C, although the amount was very small. It is expected that larger amounts of methanol may be produced by using an electrode material that is more inert than Pt/C under such conditions.

3.2. Methane oxidation over anodes comprised of non-platinum catalysts and non-carbon supports

Three anodes comprised of non-platinum catalysts and non-carbon supports, Mn_2O_3/WO_3, CrO/SnO_2, and CoO/V_2O_5, were tentatively used for methanol production. Fig. 2 shows the methanol, CO_2, and O_2 concentrations as a function of current or electrode potential at 100 °C. (Other products were not detected in the analysis.) In Fig. 2a–c, methanol, CO_2, and O_2 were produced by polarization of the anode. Common features for the three anodes were that (a) the methanol and CO_2 concentrations immediately increased by the application of current to the cell, (b) the increments in CO_2 and especially methanol concentrations were deteriorated at high currents, at which time, and (c) the O_2 concentration started to increase. These results suggest that methane is converted directly into methanol and CO_2 at low currents via Reactions (6) and (5), respectively, and that O_2 is formed at high

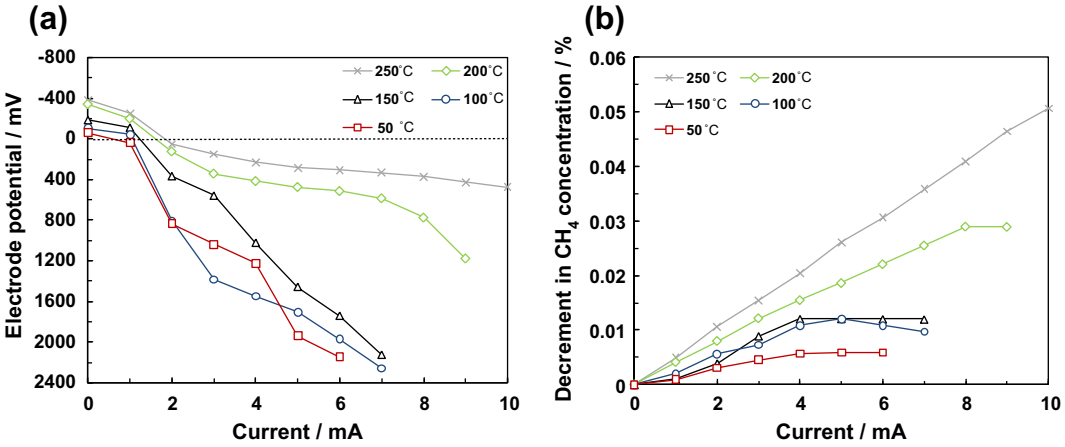

Fig. 1. Electrochemical methane oxidation over a Pt/C anode from 50 to 250 °C. (a) Potential of the anode versus the cathode and (b) decrement in methane concentration in the outlet gas from the anode chamber as a function of current.

Table 1
Product concentrations observed using the Pt/C anode and the corresponding theoretical values.

Temperature (°C)	Products at 5 mA							
	CH_3OH conc. (%)		CO_2 conc. (%)		O_2 conc. (%)		CO conc. (%)	
	Observed value	Theoretical value	Observed value	Theoretical value	Observed value	Theoretical value	Observed value	Theoretical value
50	0	0.1246	0.0059	0.0311	0.0141	0.0623	0	0.0415
100	0.0021	↑	0.0098	↑	0.0069	↑	0	↑
150	0	↑	0.0131	↑	0.0036	↑	0	↑
200	0	↑	0.0189	↑	0	↑	0	↑
250	0	↑	0.0256	↑	0	↑	0	↑

The theoretical concentrations of CH_3OH, CO_2, O_2, and CO were calculated from Faraday's law based on two-, eight-, four-, and six-electron reactions, respectively.

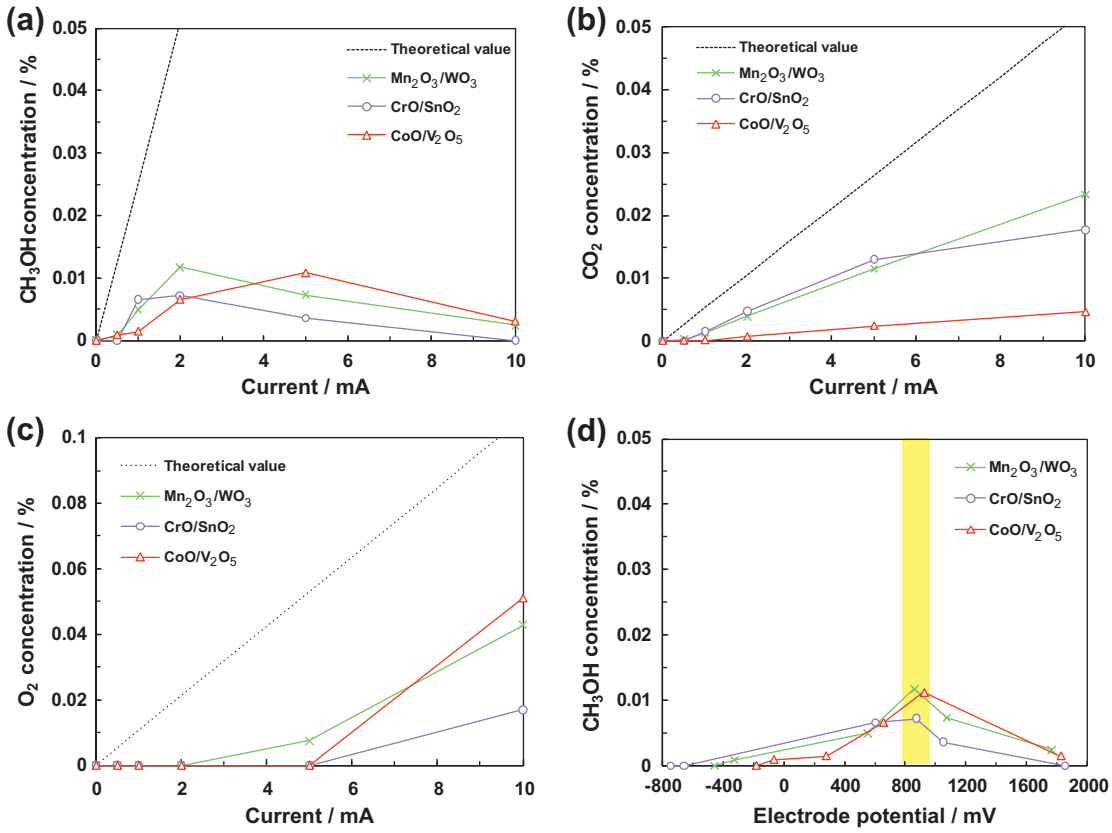

Fig. 2. Product concentrations observed using the Mn_2O_3/WO_3, CrO/SnO_2, and CoO/V_2O_5 anodes at 100 °C. (a) Methanol, (b) CO_2, and (c) O_2 concentrations as a function of current. (d) Methanol concentration as a function of anode potential.

currents via Reaction (11). Interestingly, although the three anodes showed different currents where the methanol concentration was the maximum (Fig. 3a), the methanol concentrations always reached a peak at potentials around +900 mV (Fig. 3d), which suggests a close relationship between the methanol production and the electrode potential. It is likely that formation of the active oxygen species is inhibited by excess polarization of the anode, which results in the appearance of Reaction (11), as will be discussed later. It is thus concluded that the upper limit for the applied potential is +900 mV, which corresponds to the current range of 2–5 mA, depending on the anode species.

The results provide evidence that methane can be directly oxidized to methanol by employing an anode that is more inert than Pt/C. However, while the selectivity toward methanol was over 50% at 2 mA for all of the anodes tested, the current efficiencies for methanol production were still as low as 24.6%, 14.5%, and 13.2% at 2 mA over the Mn_2O_3/WO_3, CrO/SnO_2, and CoO/V_2O_5 anodes, respectively. Therefore, we searched for more suitable supports and catalysts in an attempt to make a breakthrough with respect to the current efficiencies for methanol production.

Table 2 summarizes the methanol and CO_2 concentrations at 100 °C when a 1 wt.% Mn_2O_3 catalyst, which exhibited the best performance in the preliminary experiments, was impregnated on the surface of various supports. Very large differences in the methanol and CO_2 concentrations were observed among the supports, which indicate a strong effect of the support material on methanol and CO_2 production. This was not due to the difference in the BET surface areas of the supports, because the order of the BET surface area was not in agreement with the order found for the methanol and CO_2 concentrations using each support: the BET surfaces of SnO_2, WO_3, MoO_3, ZrO_2, Fe_2O_3, CeO_2, and TiO_2 were 4.7, 6.1, 2.1, 4.0, 5.5, 2.1, and 10.6 $m^2\ g^{-1}$, respectively. This point is discussed later. From Table 2, it can also be confirmed that the SnO_2 support provided the highest current efficiency for methanol production (33.5% at 2 mA) and selectivity toward methanol (80.7% at 2 mA). SnO_2 is also known to be an alternative candidate to carbon in polymer electrolyte fuel cells [13]. Therefore, SnO_2 was employed as the support material in subsequent experiments.

Table 2 also summarizes the methanol and CO_2 concentrations at 100 °C for various catalysts impregnated on the surface of the SnO_2 support, where the catalyst content was 1 wt.%. There were significant differences in the methanol concentrations among the catalysts, whereas the CO_2 concentrations were very similar. It seems that methanol and CO_2 are produced by different reaction paths, as will be described later. Of the catalysts examined, the V_2O_5 catalyst exhibited the highest current efficiency and methanol selectivity at 2 mA of 61.4% and 88.4%, respectively.

Next, the content of the V_2O_5 catalyst on the support was optimized, and the resultant methanol and CO_2 concentrations are shown in Fig. 3a and b, respectively. The methanol concentration increased with increasing V_2O_5 content, reached a maximum at 1 wt.% V_2O_5, and then decreased for V_2O_5 > 1 wt.%. Unfortunately, the current efficiency and methanol selectivity could not be improved; however, Fig. 3 does provide additional information that assists in the identification of the reaction mechanisms for methanol and CO_2 production. Over pure SnO_2 (0 wt.% V_2O_5 in Fig. 3), methanol was not observed as a product, but a large amount of CO_2 was detected, which demonstrates that CO_2 formation occurs over the SnO_2 support. Accordingly, the CO_2 concentration shown in the bottom columns of Table 2 was essentially independent of the catalyst species, and the CO_2 concentration shown in the upper columns of Table 2 was strongly dependent on the support species. In contrast, over pure V_2O_5 (100 wt.% V_2O_5 in Fig. 3), methanol rather than CO_2 was the main product, which indicates that meth-

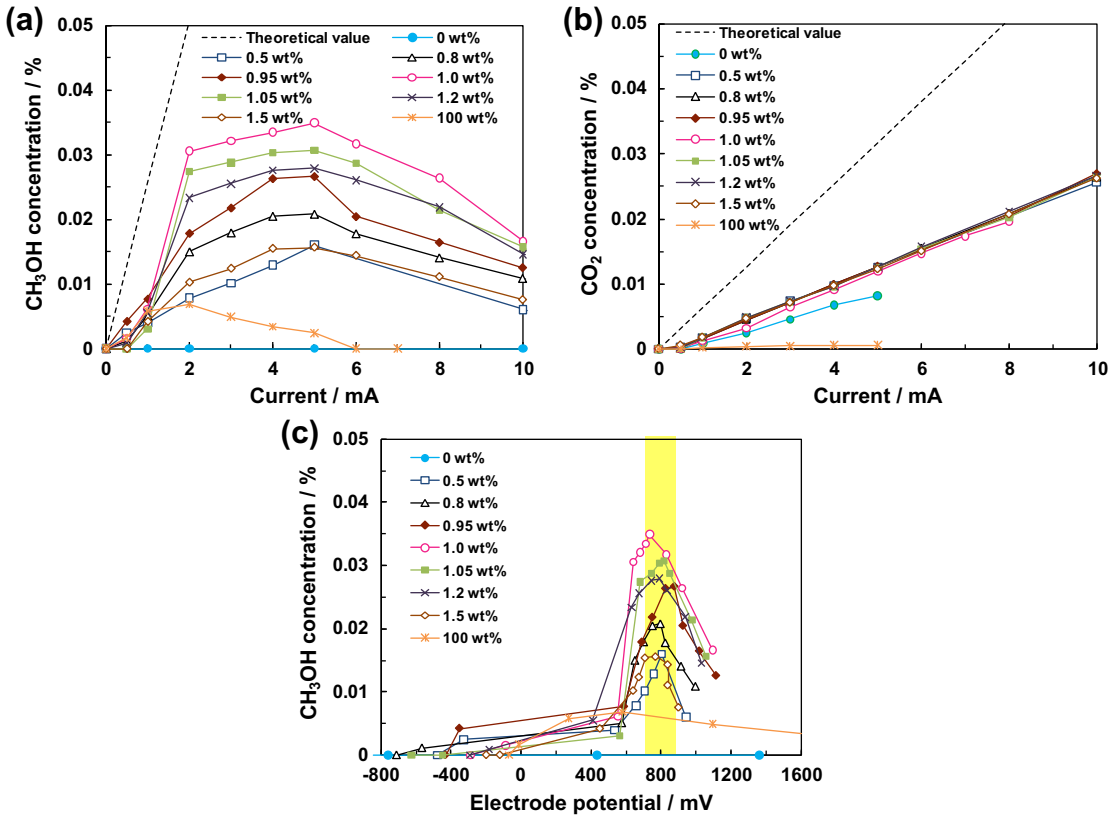

Fig. 3. Product concentrations observed using the V_2O_5/SnO_2 anode with various V_2O_5 contents at 100 °C. (a) Methanol and (b) CO_2 concentrations as a function of current. (c) Methanol concentration as a function of anode potential.

Table 2
Product concentrations observed using various non-platinum catalysts and non-carbon supports and the corresponding theoretical values.

Support	Catalyst	Products at 2 mA							
		CH_3OH conc. (%)		CO_2 conc. (%)		O_2 conc. (%)		CO conc. (%)	
		Observed value	Theoretical value	Observed value	Theoretical value	Observed value	Theoretical value	Observed value	Theoretical value
SnO_2	Mn_2O_3	0.0167	0.0498	0.0040	0.0124	0	0.0249	0	0.0166
WO_3	Mn_2O_3	0.0118	↑	0.0044	↑	0	↑	0	↑
MoO3	Mn_2O_3	0.0047	↑	0.0006	↑	0	↑	0	↑
ZrO_2	Mn_2O_3	0.0036	↑	0.0043	↑	0	↑	0	↑
Fe_2O_3	Mn_2O_3	0.0034	↑	0.0003	↑	0.0049	↑	0	↑
CeO_2	Mn_2O_3	0.0019	↑	0.0016	↑	0	↑	0	↑
TiO_2	Mn_2O_3	0.0014	↑	0.0014	↑	0.0055	↑	0	↑
SnO_2	V_2O_5	0.0306	↑	0.0040	↑	0	↑	0	↑
SnO_2	Fe_2O_3	0.0243	↑	0.0043	↑	0	↑	0	↑
SnO_2	Au	0.0191	↑	0.0045	↑	0	↑	0	↑
SnO_2	CoO	0.0173	↑	0.0023	↑	0	↑	0	↑
SnO_2	Pd	0.0168	↑	0.0041	↑	0	↑	0	↑
SnO_2	Mn_2O_3	0.0167	↑	0.0040	↑	0	↑	0	↑
SnO_2	Ru	0.0138	↑	0.0039	↑	0	↑	0	↑
SnO_2	MoO_3	0.0102	↑	0.0045	↑	0	↑	0	↑
SnO_2	Ag	0.0084	↑	0.0043	↑	0	↑	0	↑
SnO_2	CrO	0.0072	↑	0.0047	↑	0	↑	0	↑

The theoretical concentrations of CH_3OH, CO_2, O_2, and CO were calculated from Faraday's law based on two-, eight-, four-, and six-electron reactions, respectively.

anol formation occurs over the V_2O_5 catalyst. Moreover, the quantity of methanol produced was largely dependent on the V_2O_5 content, which suggests that methanol production is influenced by the structural, morphological, or redox characteristics of V_2O_5. Another important result is that the methanol concentration again reached a peak at potentials around +900 mV for all V_2O_5 contents tested (Fig. 3c), which recognizes the large effect of the electrode potential on methanol production.

Electrochemical methane oxidation was also performed under various reaction conditions, and the results are summarized as follows. (1) 100 °C was the optimal temperature for methanol production. (2) There was no significant dependence of methanol production on the methane concentration in the reactant gas, which suggests that the reaction of methane with the active oxygen species is not the rate-determining step in methanol production. (3) Methanol production was enhanced with the increase in

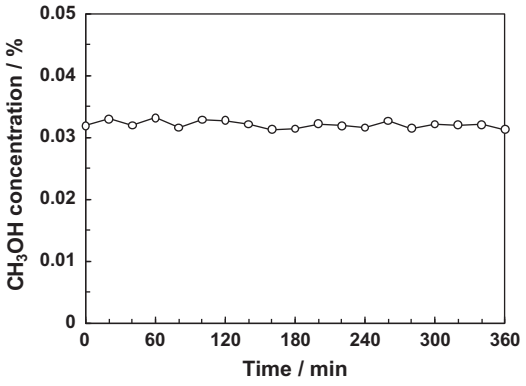

Fig. 4. Short-term stability test of methanol production over the V_2O_5/SnO_2 anode. Electrochemical methane oxidation was performed at a current of 2 mA and at a reaction temperature of 100 °C.

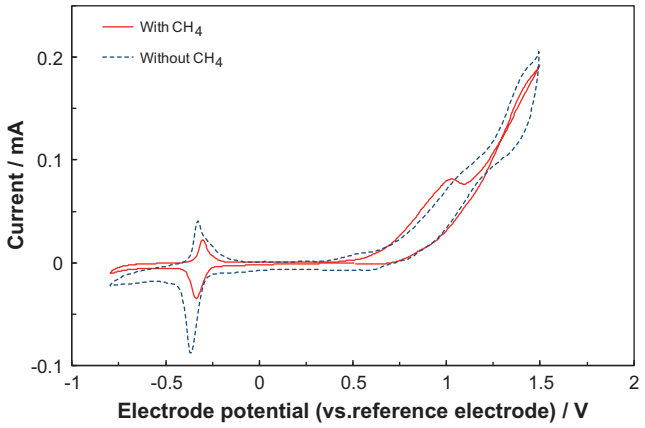

Fig. 5. CV profiles of the V_2O_5/SnO_2 anode with and without methane at 100 °C. A Au electrode was attached on the side surface of the electrolyte, which was exposed to ambient air.

H_2O vapor concentration in the reactant gas, which implies that H_2O vapor is important for the effective formation of active oxygen species for methanol production. It is also important to note that the concentration of methanol produced in the electrochemical cell at 100 °C was kept almost constant for at least 6 h, as shown in Fig. 4.

3.3. Nature of the active oxygen species formed over V_2O_5/SnO_2

CV measurements are useful to further clarify the mechanism for methanol production over the V_2O_5/SnO_2 anode. Fig. 5 shows a CV curve of the anode in a feed mixture of methane and H_2O, in addition to data in the absence of methane for comparison. In the two CV curves, the peaks at potentials between −0.3 and −0.4 V are associated with hydrogen adsorption/desorption on the catalyst surface. Importantly, a small anodic peak between +850 and +1000 mV was observed during anodic polarization in the presence of methane. The presence of this peak is attributed to the formation of the active oxygen species that is assumed to oxidize methane to methanol. Further anodic polarization oxidizes the active oxygen species to atomic or molecular oxygen, which is assumed to be inactive toward methane oxidation, and thus, the anodic current decreases at approximately +1200 mV. The results also correspond well to those shown in Figs. 2d and 3c.

To gain further clarification into the formation of the active oxygen species over the V_2O_5/SnO_2 anode, the electrode sample was characterized using various analysis techniques. No crystalline V_2O_5 was detected in the XRD pattern (Fig. 6a). For the supported V_2O_5 catalyst, it is well established that crystalline V_2O_5 is formed above monolayer surface coverage [14]. Only spherical-shaped SnO_2 crystals with diameters of 60–120 nm were observed by TEM (Fig. 6b). However, EDX analysis of Position 1 in the TEM image confirmed that the composition of the crystals was multi-component and contained both Sn and V. Similar results were observed at other positions. Moreover, the V $2p_{3/2}$ XPS spectrum had two separated peaks, which indicates the presence of V^{5+} and V^{4+} (Fig. 6c). The concentration ratio of $V^{4+}/(V^{5+} + V^{4+})$ estimated from the relative peak areas for the V $2p_{3/2}$ spectrum was 0.34, which is much higher than the concentration ratio of 0.08 for pure V_2O_5. These analytical observations are indicative of the presence of highly dispersed and partially reduced vanadium species on the SnO_2 surface.

The identification of the active oxygen species still remains unclear at the present time. However, different anion radicals such as O_2^- and $O^{\cdot -}$ have been formed over partially reduced V_2O_5-based catalysts [15,16]. These oxygen species also exhibit high reactivity for partial oxidation of hydrocarbons at intermediate temperatures [17]. Therefore, we speculate that these anion radicals are electrochemically generated over V^{4+} sites according to Reactions (12) and (13).

$$H_2O \rightarrow O^{\cdot -} + 2H^+ + e^- \quad (12)$$

$$2H_2O \rightarrow O_2^- + 4H^+ + 3e^- \quad (13)$$

Based on the experimental results of this study, it is also reasonable to consider that these reactions are most significant at an electrode potential of approximately +900 mV. In addition, the chemisorption of methane most likely requires twin vanadium–oxygen species [18]. Consequently, for effective methanol production, it is necessary to increase the concentration of V^{4+} sites. In an early electron paramagnetic resonance (EPR) study, a large quantity of V^{4+} sites were reported to be formed on the surface of a SnO_2 support by incorporating a portion of the Sn^{4+} ions into V_2O_5 [19]. This may be a major reason that SnO_2 was notably the best support in this study. At the same time, however, the use of this support promotes the formation of CO_2, as described earlier. It is likely that the generation of highly active oxygen species, probably OH· radicals, is enhanced over SnO_2, similarly to that over Pt and carbon. (Yamanaka et al. reported that the OH· radical attacks the C–H bond of methane and then oxidation results in the production of mainly CO_2 [20].) Therefore, further research is required in catalyst development to improve the current efficiency for methanol production.

4. Conclusions

A new scheme for direct methane oxidation to methanol was proposed using a fuel cell-type reactor. The current efficiency for methanol production and selectivity toward methanol were evaluated, and the reaction mechanism was discussed with respect to the generation of active oxygen species over catalyst active sites.

(1) Electrochemical methane oxidation was first inspected over a Pt/C anode in a feed mixture of methane and H_2O vapor at various temperatures. The methane concentration was decreased with the increase in current, the extent of which became larger as the temperature increased. However, CO_2 and O_2 were the major products, where CO_2 concentration increased with increasing temperature, while the O_2 concentration decreased.

(2) Various electrodes comprised of non-platinum catalysts and non-carbon supports were investigated as anodes for methanol production. The production of methanol over the $V_2O_5/$

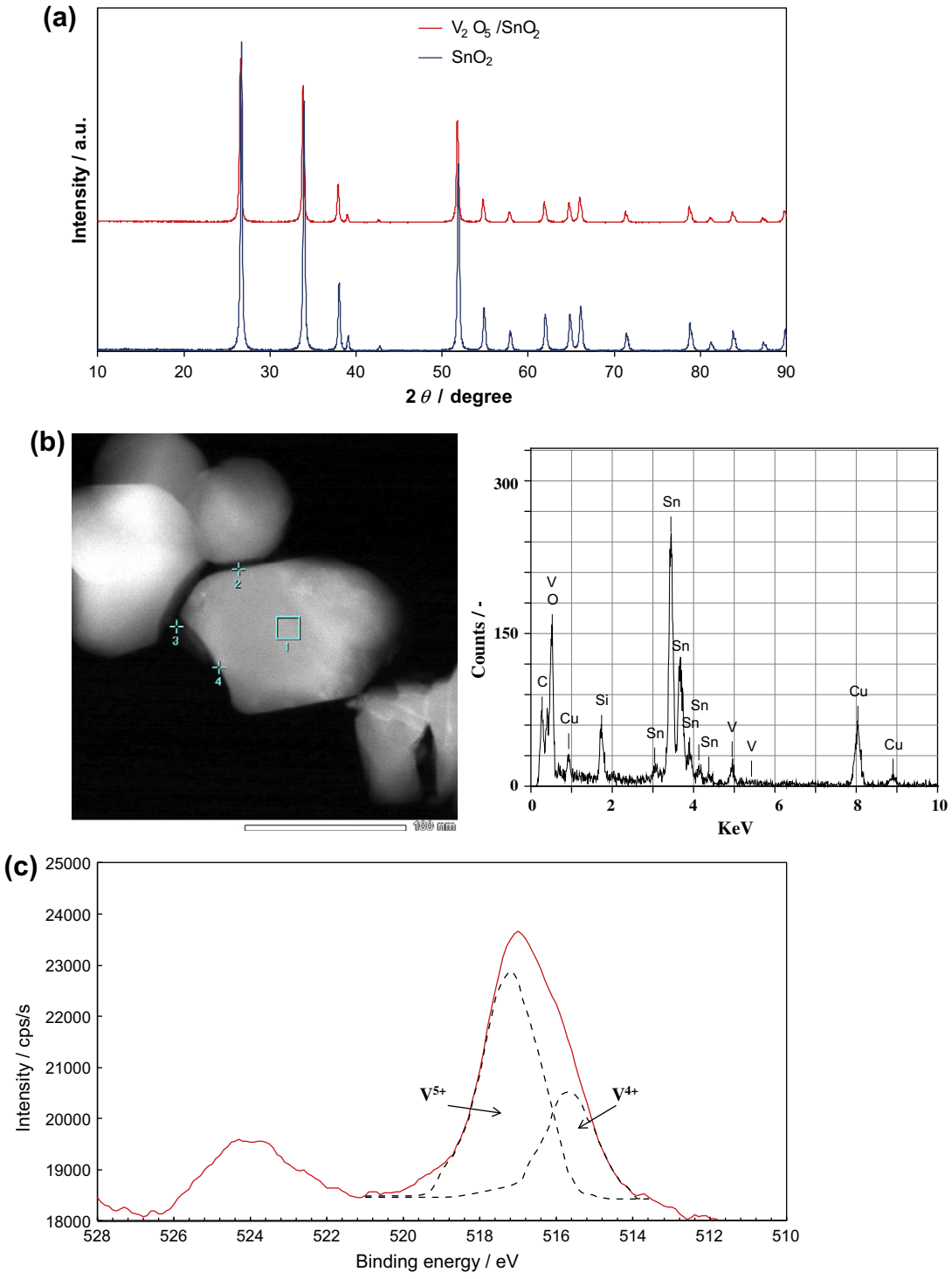

Fig. 6. (a) XRD pattern, (b) TEM image and EDX spectrum, and (c) XPS spectrum of the V_2O_5/SnO_2 electrode.

SnO_2 anode was the most significant among the anodes tested. The resultant current efficiency for methanol production and selectivity toward methanol reached 61.4% and 88.4%, respectively, at 100 °C. Another important result is that the methanol production reached a peak at potentials around +900 mV, which indicates a close relationship between methanol production and the electrode potential.

(3) The V_2O_5/SnO_2 anode was characterized using XRD, TEM, and XPS measurements. The vanadium species were observed to be highly dispersed and partially reduced on the SnO_2 surface. Active oxygen species that oxidize methane to methanol were concluded to be generated by the anodic polarization of H_2O vapor over V^{4+} sites at potentials around +900 mV.

References

[1] N.D. Spencer, J. Catal. 109 (1988) 187.
[2] Z. Sojka, R.G. Herman, K. Klier, J. Chem. Soc. Chem. Commun. (1991) 185.
[3] A. Parmaliana, F. Frusteri, A. Mezzapica, M.S. Scurrel, N. Giordano, J. Chem. Soc. Chem. Commun. (1993) 751.

[4] T. Kobayashi, K. Nakagawa, K. Tabata, M. Haruta, J. Chem. Soc. Chem. Commun. (1994) 1609.
[5] A. de Lucas, J.L. Valverde, P. Canizares, L. Rodriguez, Appl. Catal. A: Gen. 184 (1999) 143.
[6] A. Tomita, J. Nakajima, T. Hibino, Angew. Chem. Int. Ed. 47 (2008) 1462.
[7] B. Lee, Y. Sakamoto, D. Hirabayashi, K. Suzuki, T. Hibino, J. Catal. 271 (2010) 195.
[8] P. Heo, K. Ito, A. Tomita, T. Hibino, Angew. Chem. Int. Ed. 47 (2008) 7841.
[9] E. Passalacqua, P.L. Antonucci, M. Vivaldi, A. Patti, V. Antonucci, N. Giordano, K. Kinoshita, Electrochim. Acta 37 (1992) 2725.
[10] B. Scharifker, O. Yépez, J.C. De Jesús, M.M. Ramírez de Agudelo, US Patent No. 5051,156, 1991.
[11] M. Nagao, A. Takeuchi, P. Heo, T. Hibino, M. Sano, A. Tomita, Electrochem. Solid-State Lett. 9 (2006) A105.
[12] Y.C. Jin, Y.B. Shen, T. Hibino, J. Mater. Chem. 20 (2010) 6214.
[13] T. Okanishi, T. Matsui, T. Takeguchi, R. Kikuchi, K. Eguchi, Appl. Catal. A 298 (2006) 181.
[14] A.M. Turek, I.E. Wachs, E. DeCanio, J. Phys. Chem. 96 (1992) 5000.
[15] V.A. Shvets, V.M. Vorontinzev, V.B. Kazansky, J. Catal. 15 (1969) 214.
[16] B.N. Shelimov, C. Naccache, M. Che, J. Catal. 37 (1975) 279.
[17] G. Centi, F. Trifiro, J.R. Ebner, V.M. Franchetti, Chem. Rev. 88 (1988) 55.
[18] K.J. Zhen, M.M. Khan, C.H. Mak, K.B. Lewis, G.A. Somorjai, J. Catal. 94 (1985) 501.
[19] F. Okada, A. Satsuma, A. Furuta, A. Miyamoto, T. Hattori, Y. Murakami, J. Phys. Chem. 94 (1990) 5900.
[20] I. Yamanaka, S. Hasegawa, K. Otsuka, Appl. Catal. A 226 (2002) 305.